Biosensors and Bioelectronics 188 (2021) 113339

Contents lists available at ScienceDirect

Biosensors and Bioelectronics

journal homepage: www.elsevier.com/locate/bios

Investigation of colorimetric biosensor array based on programable surface chemistry of M13 bacteriophage towards artificial nose for volatile organic compound detection: From basic properties of the biosensor to practical application

Jong-Min Lee [a,1], Yujin Lee [b,1], Vasanthan Devaraj [a,1], Thanh Mien Nguyen [b], Ye-Ji Kim [b], You Hwan Kim [c], Chuntae Kim [a], Eun Jung Choi [a,*], Dong-Wook Han [a,d,**], Jin-Woo Oh [a,b,c,***]

[a] Bio-IT Fusion Technology Research Institute, Pusan National University, Busan, 46241, Republic of Korea
[b] Department of Nano Fusion Technology, Pusan National University, Busan, 46241, Republic of Korea
[c] Department of Nanoenergy Engineering, Pusan National University, Busan, 46241, Republic of Korea
[d] Department of Cogno-Mechatronics Engineering, Pusan National University, Busan, 46241, Republic of Korea

ARTICLE INFO

Keywords:
Bioelectronic nose
Bacteriophage
Genetic engineering
Biomaterials
Surface chemistry

ABSTRACT

Various threats such as explosives, drugs, environmental hormones, and spoiled food manifest themselves with the presence of volatile organic compounds (VOCs) in our environment. In order to recognize and respond to these threats early, the demand for highly sensitive and selective electronic noses is increasing. The M13 bacteriophage-based optoelectronic nose is an excellent candidate to meet all these requirements. However, the phage-based electronic nose is still in its infancy, and strategies that include a systematic approach and development are still essential. Here, we have integrated theoretical and experimental approaches to analyze the correlation between the surface chemistry of genetically engineered phage and the phage-based optoelectronic nose properties. The reactivity of the genetically engineered phage color film to some VOCs were quantitatively analyzed, and the correlation with the binding affinity value calculated by Density-functional theory (DFT) was compared. This demonstrates that phage color films have controllable reactivity through a genetic engineering. We have selected phages that are advantageous in distinguishing each VOCs in this work through hierarchical cluster analysis (HCA). The reason for this difference was verified through the optimized geometry calculated by DFT. Through this, it was confirmed that the tryptophan-based and the Histidine-based of genetically engineered phage film are important in distinguishing the VOCs (Y-hexanolactone, 2-isopropyl-4-methylthiazole, ethanol, acetone, ethyl acetate, and acetaldehyde) used in this work to evaluate the peach freshness quality. This was applied to the design of a field-applied phage-based optoelectronic nose and verified by measuring the freshness of the actual fruit.

1. Introduction

Detecting volatile organic compounds (VOCs) in the field, including VOCs such as drugs, explosives, hazardous chemicals, and odor caused by putrefaction, is always complex and noisy (Laurent, 2002). For example, ethylene gas resulting from spoilage of fruit does not exist in isolation but is mixed with fruit flavor molecules (Li and Suslick, 2019). Therefore, on-site volatile organic compounds (VOC) detection systems must display high sensitivity and excellent selectivity along with high resolution. In order to achieve this set of goals, technologies for detecting and monitoring various VOCs are being actively developed. Gas chromatography-mass spectrometry (GC-MS) is an excellent technology for analyzing components of a mixture, including detecting and quantifying trace components in various environmental samples

* Corresponding author.
** Corresponding author. Bio-IT Fusion Technology Research Institute, Pusan National University, Busan, 46241, Republic of Korea.
*** Corresponding author. Bio-IT Fusion Technology Research Institute, Pusan National University, Busan, 46241, Republic of Korea.
E-mail addresses: eunjung721203@gmail.com (E.J. Choi), nanohan@pusan.ac.kr (D.-W. Han), ojw@pusan.ac.kr (J.-W. Oh).
[1] These authors contributed equally to this work.

https://doi.org/10.1016/j.bios.2021.113339
Received 19 April 2021; Received in revised form 10 May 2021; Accepted 11 May 2021
Available online 16 May 2021

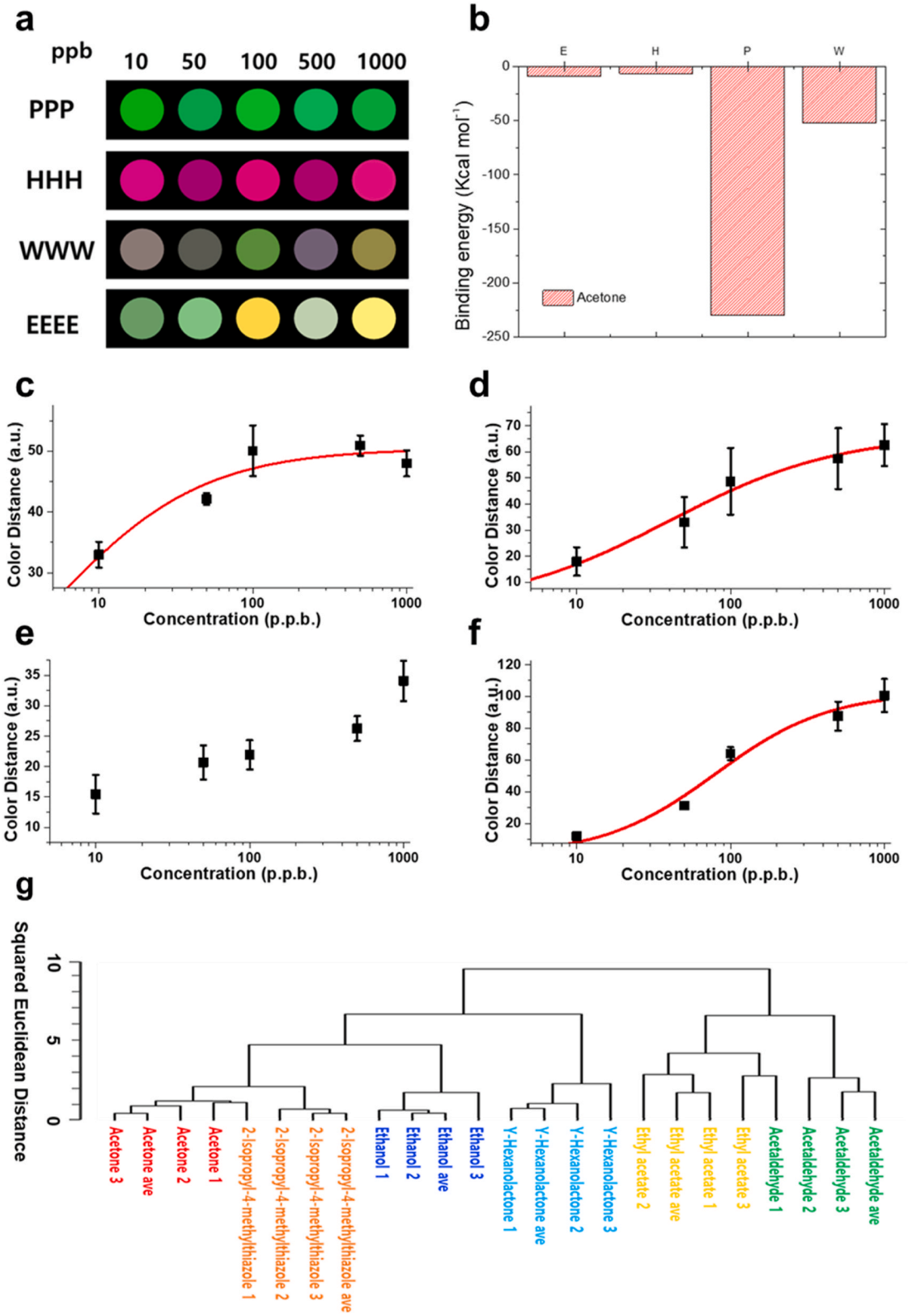

Fig. 1. Phage color film measurement results and analysis for acetone. (a) Color difference pattern based on acetone concentration (10, 50, 100, 500, 1000 ppb). (b) Binding affinities of acetone for the four tested amino acids as calculated from DFT simulations. (c–f) Color distances of acetone detection with genetically engineered phage color films were each fitted with the Hill equation to obtain dissociation constant (Kd) values. Please see Table S1 for raw data, standard deviations, and standard errors. The obtained Kd values were (c) 5.05 for the PPP-type, (d) 39.78 for the HHH-type, (e) fitting fail for the WWW-type, and (f) 80 for the EEEE-type. (g) Classification dendrogram of VOCs at 1000 ppb. (For interpretation of the references to color in this figure legend, the reader is referred to the Web version of this article.)

(Giannoukos et al., 2016; Santos and Galceran, 2003; Yu et al., 2020). Ion mobility spectrometry (IMS) also displays excellent sensitivity and resolution, and detection of toxic gases, explosives, and drugs are widely known applications of this technique (Ewing, 2001; Caygill et al., 2012). However, the large sizes and high prices of these devices remain a considerable hurdle. There is a demand to develop an alternative portable technology (in addition to use it without an auxiliary equipment) which is capable of detecting in real time a target material.

Several sensor device technologies have been proposed for VOCs measurement (Yang et al., 2017; Murugathas et al., 2019, 2020; Kwon et al., 2019; Lee et al., 2020). Among them, color sensors are emerging as a possible alternative technology due to its simplicity and convenience. The color sensor is a technology that recognizes the target material by changing its color (Liu et al., 2020; Hu et al., 2020). A distinct advantage of color sensors is that they can provide real-time information in the field with the naked eye. Litmus paper is the most representative color sensor. It is capable of immediately determining a physicochemical property qualitatively in any place using only the color change. The self-pregnancy test kit is also an example of a color sensor. In the field of "optoelectronic noses", the results of the Suslick group have been impressive: they reported the ability to successfully classify a variety of subjects, starting with VOCs, alcohols, soda drinks, and foods (Janzen et al., 2006; Zhang et al., 2006; Zhang and Suslick, 2007; Suslick et al., 2010; Lin et al., 2011; Li and Suslick, 2018, 2019). However, the ability of sensors based on chemical reactions (e.g., devices involving dyes) to function for a long time can be seriously undermined by external mechanical and chemical factors.

To overcome these limitations, our group has developed color sensors based on the M13 bacteriophage (phage). The fundamental mechanism behind the phage color sensor relies on its structural color appearing as an array of nanometer-scale optical cavities (Kinoshita and Yoshioka, 2005). The structure of this phage is that of a nanofiber with a very high surface-to-volume ratio, with about 2700 copies of protein VIII (pVIII) on the surface per particle and 4 to 5 copies of proteins (pIII, protein VIII) on both ends of each particle (Marvin et al., 2006). The structure of the nanofiber is dense, a feature advantageous in endowing the fiber with good resistance to mechanical damage and thermal damage. A desired peptide can be expressed on each corresponding surface protein by appropriately controlling the genes in the bacteriophage (Merzlyak et al., 2009; Parmley and Smith, 1989; Scott and Smith, 1990; Tian et al., 2004; Liu et al., 2008). Combining the 20 naturally encoded amino acid residues on the surface of a phage allows for the creation of a rich variety of genetically engineered phages with distinct surface chemistries but still retaining the same overall morphology. Phage display is an evolutionary screening method for developing an M13 phage that specifically binds to a desired material (Smith and Petrenko, 1997; Smith, 1985). Based on this technique, a tryptophan-Histidine-tryptophan (WHW) type phage selective for trinitrotoluene (TNT) has been developed (Oh et al., 2014). In addition, a phage color sensor has been developed that detects various targets such as environmental hormones, in particular endocrine-disrupting chemicals (Moon et al., 2016). However, these sensors have so far been only tested successfully in a laboratory environment, and their measurements in the field have been insufficiently reliable.

In developing an efficient phage-based electronic nose, it is vital to investigate the effect of surface chemistry of a genetically manipulated phage on the responsiveness of the phage-based color sensor. Also, the intended modification in the genetically engineered phage is verified through DNA sequencing (Oh et al., 2014; Yoo et al., 2020). Although this method is highly reliable, information on reactivity with foreign substances cannot be obtained. Direct determination of the surface chemical properties of phages has been carried out using chemical reactions in solution (Lee et al., 2019). This method is very reliable, but only applicable if the target material is solution-based. In other words, limitation in detecting VOCs still remain. Verification of surface chemical properties in genetically engineered phage-based color sensors is necessary because it includes variables that may appear in mass culture and self-assembly processes. In addition, the reactivity of the phage color film is not only affected by the surface chemistry of phage, but also the bundle size (length of the bio-nano optical cavity). Therefore, it is necessary to analyze the quantitative reactivity or selectivity of the phage color film itself.

Here, we constructed a portable detection system capable of doing field tests based upon different reactivity exhibited by the programmable surface chemistry of a genetically engineered M13 phage. The main surface protein's sequences (pVIII) of the genetically engineered phages used were: Pro-Pro-Pro (PPP), His-His-His (HHH), Trp-Trp-Trp (WWW), and Glu-Glu-Glu-Glu (EEEE or 4E). Genetically engineered phage-based color films were fabricated into nanostructures showing structural colors through solution-based self-assembly, like for our previous results (Please see "Materials and method" section in Supporting Material & Fig. S1). The correlation between the phage surface chemistry and the reactivity of the color sensor was experimentally verified. This sophisticated surface chemistry manipulation allowed for a systematic approach to designing an electronic "nose". Peach freshness measurements were taken as a proof of concept. To measure peach freshness, it was necessary to endeavor to detect subtle differences in spoilage gases in a complex and noisy environment (Bleecker and Kende, 2000). An appropriate electronic nose was constructed by measuring and analyzing standard substances related to the peach flavor and to the peach decay process. The selective phage-based optoelectronic nose was confirmed to be able to classify the freshness of peaches.

2. Results and discussion

2.1. Correlation analysis between phage surface chemistry and color sensor properties

In the current work, the genetically engineered phages were each made to be identical to the wild-type phage except for 3 or 4 peptides at the pVIII terminus, with these peptides affecting the phage-based color film reactivity significantly due to their protruding to the outside. It has been reported that the reactivity of the phage-colored film is significantly increased in TNT when three peptide sequences at the pVIII end are genetically engineered with a highly selective WHW polypeptide sequence for TNT (Oh et al., 2014). d Acetone generally does not interact well with any of the tested phages (Fig. S4). This is because phage is highly hydrophilic, and acetone has non-polar methyl groups. Therefore, the results of molecular simulation of the functional peptide with acetone indicated a high binding affinity of the non-polar proline (P) peptide for acetone (Fig. 1b).

Compared to the P peptide, the other three tested peptides, i.e., those with glutamic acid (E), H, and W, respectively, were determined to bind acetone with relatively low affinity. Acetone concentration-dependent color distance was measured to confirm that these chemical properties were present in the phage color sensor (Fig. 1a). The color distance of each genetically engineered phage-based color film increased and then became saturated with increasing acetone concentration. By fitting the Hill function to these data, dissociation constant (Kd) values of each phage-based sensor were obtained (Fig. 1c–f). The resulting Kd value of the P-type phage color sensor was the lowest, consistent with the predictions of molecular simulations. Thus the trend of the results obtained using the genetically engineered phage-based color sensors was consistent the trend of the surface chemical properties of the functional peptides. This allows quantitative evaluation and analysis of reactivity and selectivity for phage films with manipulated surface chemistry.

2.2. VOC detection and analysis

To develop a phage-based bio-optoelectronic nose applicable in the field in real time, verification of classification characteristics of VOCs occurring in the environment becomes necessary. Through this analysis,

a

	>75% Successful Classification	> 80% Confusion	Classification Success Rate (%)
PPP-HHH-WWW-EEE	Ethanol Y-Hexanolactone		92.9
WWW-EEE	Acetaldehyde Acetone		78.6
WWW-HHH	Ethanol Y-Hexanolactone		92.9
WWW-PPP	Ethanol		75
PPP-HHH	Ethanol Y-Hexanolactone	Acetone / 2-Iso-4-methyl Acetaldehyde / Ethyl acetate	75
PPP-EEE	Acetaldehyde	Ethanol / 2-Iso-4-methyl	71.4
HHH-EEE	Y-Hexanolactone	Ethanol / 2-Iso-4-methyl	75

b

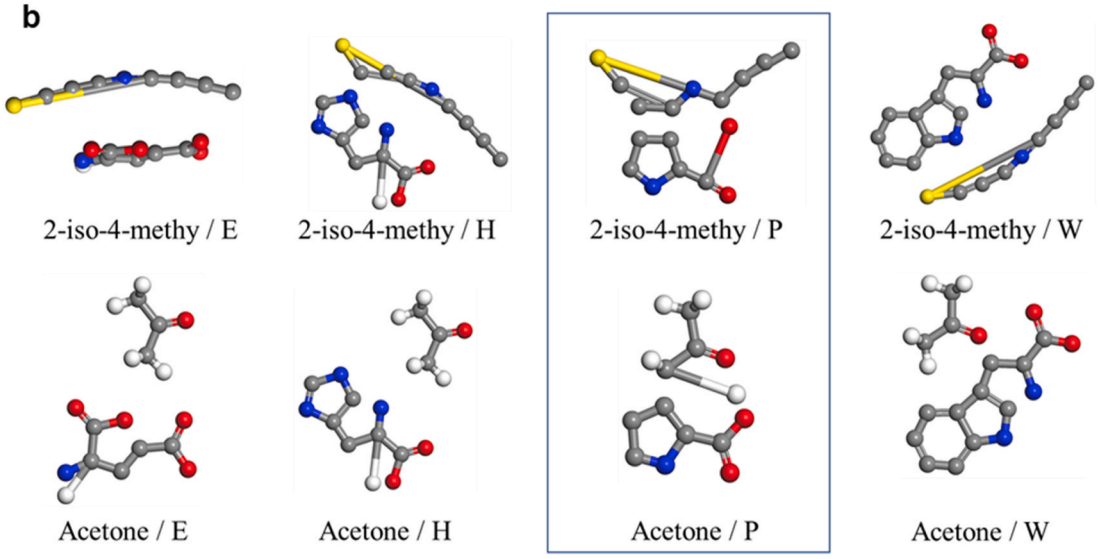

Fig. 2. Table of electronic nose properties and DFT-calculated geometry optimization. (a) Classification success rates (CSRs) of phage-based optoelectronic noses. All values were calculated based on the HCA classification method. HCA dendrograms in this table can be seen in Fig. S12. (b) Calculated optimized geometries of complexes of amino acids (E, H, P, W) and target molecules (2-iso-4-methyl, acetone). The color of atoms are as follows: carbon (grey), nitrogen (blue), oxygen (red), sulfur (yellow), and hydrogen (white). (For interpretation of the references to color in this figure legend, the reader is referred to the Web version of this article.)

the selectivity of the electronic nose can be estimated. The following five VOCs were selected for peach freshness: Y-hexanolactone (also called gamma-caprolactone), 2-isopropyl-4-methylthiazole (abbreviated here as 2-iso-4-methyl), ethanol, acetone, ethyl acetate, and acetaldehyde (Zhu and Xiao, 2019; Song et al., 1997; He et al., 2021). Y-Hexanolactone and 2-iso-4-methyl are representative substances with high concentrations measured using GC-MS in the reference related to peaches. Y-Hexanolactone is found in many fruits, including peaches, and has a sweet smell. 2-Iso-4-methyl is a substance used in fruit and vegetable flavors. Ethanol, acetone, ethyl acetate, and acetaldehyde are VOCs released during fruit ripening. They influence the flavor, freshness, ripeness, and quality of the fruit. The same method used for the analysis of acetone was also used in the current work for the remaining 4 VOCs (see Figs. S5–S8 for Kd values & Table S1 for raw data).

To confirm the effect of the surface chemistry of each genetically engineered phage on its electronic nose properties, the analysis was performed by using various combinations of the tested peptides, as listed in Fig. 2a. As with our previous report, Hierarchical Cluster Analysis (HCA) results were quantitatively evaluated and expressed as classification success rates (CSRs) (Park et al., 2021). In the previous report, the

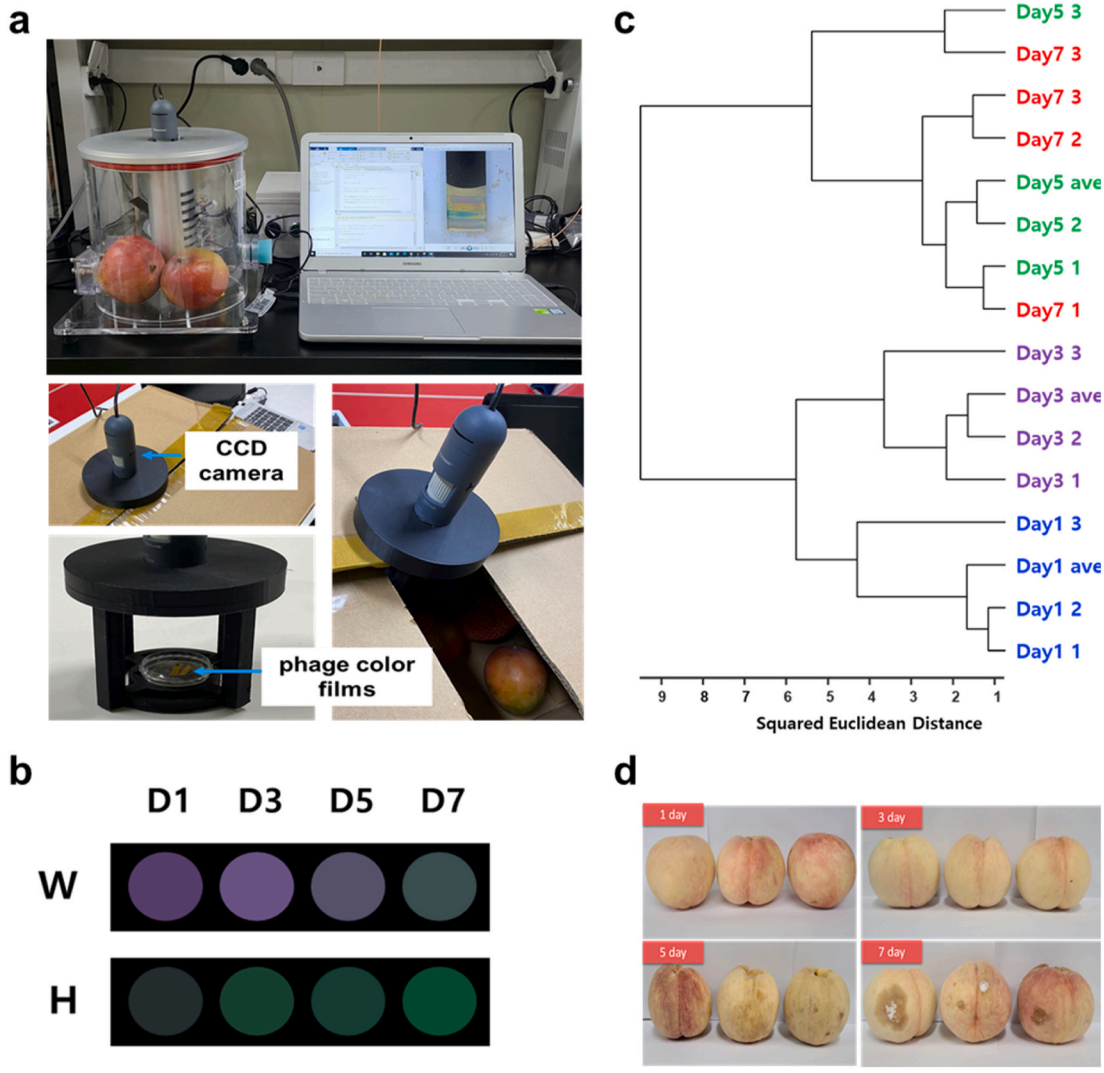

Fig. 3. Actual sample measurements. (a) Photographs composed of a phage-based bioelectronic nose composed of phage color films of 2 cm × 2 cm and a CCD camera. (b) Color difference pattern. Please see Fig. S14 for raw data. (c) Freshness monitoring result by storage time. (d) Photographs of peaches taken at the indicated numbers of days of storage. Decay was observed starting at 5 days after storage. (For interpretation of the references to color in this figure legend, the reader is referred to the Web version of this article.)

reactivity and selectivity of genetically engineered phage-colored films were not quantitatively analyzed. So it is difficult to extend to the general discussion about phage electron nose design strategy. On the other hand, in this work, the quantitative analysis approach can provide a guideline for effective phage-based electronic nose design. High CSRs were found when W and H were used (Fig. 1g) but low values were found for P and E—with low CSR values (Fig. S12) indicating poor classification of the VOCs and possible confusion of the VOCs with one another. Interestingly, W and H display the most dramatic differences in Kd values (Fig. 1c–f and S6-S8) among the five quantitatively analyzed VOCs. Since the detection performance of electron noses is based on cross-reactive receptors, the combination of the most dramatic differences in reactivity and selectivity is advantageous. A confusion rate of more than 80% was considered to indicate an inability of the electronic nose to distinguish between the two VOCs.

Molecular structure optimization calculations were performed (Fig. 2b) to determine why certain amino acids on HCA led to VOCs being confused for one another. In particular, P-type and H-type phage-based optoelectronic noses were not able to distinguish between acetone and 2-iso-4-methyl. The particularly poor ability of the P-type to classify VOCs may have been due to the considerable difference between the geometry of P and the geometries of other amino acids. For example, while acetone and 2-iso-4-methyl were calculated to bind to the same side of P, they were calculated to bind to opposite faces of W. Also, for H and E, there was a considerable difference between the stabilized geometries for acetone and 2-iso-4-methyl: in the case of E, the coordinate planes of acetone and 2-iso-4-methyl differed; and in the case of H, the nearest positions significantly differed. Due to electron interactions differing depending on the stabilization geometry, W, H, and E-type phages were expected to exhibit significantly different responses to acetone and 2-iso-4-methyl. This other reaction was interpreted to greatly influence the classification characteristics in the phage-based electronic nose. In the case of P, acetaldehyde and ethyl acetate were poorly discriminated, explaining the low CSR of the phage-based photoelectronic nose containing the P-type phage as a whole. For E, the ability to distinguish ethanol from 2-iso-4-methyl was also poor, attributed to the difference between their optimized geometries. The same characteristics were observed in the case of acetaldehyde/ethyl acetate and ethanol/2-iso-4-methyl, where the phage optoelectronic nose confused them by more than 80% (Figs. S9 and S10).

2.3. Peach freshness monitoring

Peach freshness was monitored by analyzing the actual change in

peach flavor over time (Fig. 3a). Peaches were monitored while being stored at room temperature in a fruit storage box, and there was no significant change in tested environmental factors, namely temperature and humidity, and in the sample sugar content during that period (Fig. S11). The phage-based electronic nose used here was composed of W and H-type phages previously selected by analyzing VOCs related to peach flavor. Measurements were taken 1, 3, 5, and 7 days after storage. Fig. 3b shows the colors of each of the phage films for various storage times (see Fig. S14 for raw data). The W-type phage-based color film darkened with time, while the H-type film became brighter—a beneficial combination of properties for an electronic nose. HCA analysis confirmed the classification according to the change in peach freshness (Fig. 3c). The results for the first and third days showed successful classification, and the results for the fifth and seventh days were mixed in a category. Significant freshness changes were visually observed from the fifth day onward (Fig. 3d), which was also indicated according to the electronic nose analysis.

Interestingly, the measured values on the first day were entirely distinct from those of the third day. The electronic nose appeared to have reacted sensitively to a slight change in scent even before the onset of decay. The analysis was performed by including the P and E-type phages used for measuring VOCs previously (Fig. S13). In this case, the measured values were found to not be classified well by storage time and the measured values were mixed. In particular, PPP-EEEE, which showed the worst CSR in the VOC analysis, exhibited flawed properties even for actual peaches. Therefore, our results confirmed that an actual phage-based optoelectronic nose could be designed based on analysis using VOCs in a laboratory environment. In addition, we also tested the physical and chemical stability of the phage-based electronic nose. In both scenarios, our device's functionality did not deteriorate irrespective of external factors, which we believe as an essential thing when considering its implementation into real-time applications (see Figs. S2 and S3; Oh et al., 2014).

3. Conclusions

Field applicable real-time monitoring phage-based bioelectronic nose has been developed in this work, emphasizing the importance of precise distinguishability and selectivity in VOCs classification. From critical insights of computational results and its deployment in genetic engineering, we specifically designed phage's surface chemistry co-relating VOC's responsiveness utilized in this work. Our phage-based electronic nose demonstrated a clear distinguishability in various stages of fruit (peach) freshness conditions like ripening, flavor, and decay state by such design developments. The enhanced classification success rate of 92.9% with precise selectivity is scored, emphasizing our design's importance alongside better device stability. This study reveals such higher classification success rates were achieved through a quantitative analysis of the reactivity of the phage color film with controlled surface chemistry. We believe the phage-based electronic nose reported in this work will function in various complex and noisy natural environments with excellent classification properties. We expected this kind of development in the electronic noses would provide critical design insights that open up its applicability in a broad range of odor-based sensors.

CRediT authorship contribution statement

Jong-Min Lee: Writing – original draft, Methodology, Investigation, Formal analysis. **Yujin Lee:** Formal analysis, Methodology, Investigation. **Vasanthan Devaraj:** Writing - Review & Editing, Validation, Software. **Thanh Mien Nguyen:** Validation, Investigation. **Ye-Ji Kim:** Formal analysis. **You Hwan Kim:** Software. **Chuntae Kim:** Validation. **Eun Jung Choi:** Resources, Methodology. **Dong-Wook Han:** Supervision, Funding acquisition. **Jin-Woo Oh:** Supervision, Project administration, Funding acquisition.

Declaration of competing interest

The authors declare that they have no known competing financial interests or personal relationships that could have appeared to influence the work reported in this paper.

Acknowledgements

This work was supported by the Korea Institute of Planning and Evaluation for Technology in Food, Agriculture and Forestry (IPET) through the Advanced Production Technology Development Program, funded by the Ministry of Agriculture, Food and Rural Affairs (MAFRA) (318104–3). This work was also supported by the National Research Foundation of Korea (NRF) grant funded by the Korea government (MSIT) (No. 2019R1A4A1024116).

Appendix A. Supplementary data

Supplementary data to this article can be found online at https://doi.org/10.1016/j.bios.2021.113339.

References

Bleecker, A.B., Kende, H., 2000. Annu. Rev. Cell Dev. Biol. 16, 1–18.
Caygill, J.S., Davis, F., Higson, S.P.J., 2012. Talanta 88, 14–29.
Ewing, R., 2001. Talanta 54, 515–529.
Giannoukos, S., Brkić, B., Taylor, S., Marshall, A., Verbeck, G.F., 2016. Chem. Rev. 116, 8146–8172.
He, K., Bu, T., Zhao, S., Bai, F., Zhang, M., Tian, Y., Sun, X., Dong, M., Wang, L., 2021. Food Chem. 129583.
Hu, M.-L., Razavi, S.A.A., Piroozzadeh, M., Morsali, A., 2020. Inorg. Chem. Front. 7, 1598–1632.
Janzen, M.C., Ponder, J.B., Bailey, D.P., Ingison, C.K., Suslick, K.S., 2006. Anal. Chem. 78, 3591–3600.
Kinoshita, S., Yoshioka, S., 2005. ChemPhysChem 6, 1442–1459.
Kwon, O.S., Song, H.S., Park, T.H., Jang, J., 2019. Chem. Rev. 119, 36–93.
Laurent, G., 2002. Nat. Rev. Neurosci. 3, 884–895.
Lee, J.-M., Choi, E., Park, J., Devaraj, V., Kim, C., Han, J., Kim, W.-G., Kim, Kyujung, Kang, Y.-C., Kim, Kwang, Oh, J.-W., 2019. Viruses 11, 248.
Lee, S.H., Lee, M., Yang, H., Cho, Y., Hong, S., Park, T.H., 2020. Biosens. Bioelectron. 154, 112071.
Li, Z., Suslick, K.S., 2018. ACS Sens. 3, 121–127.
Li, Z., Suslick, K.S., 2019. Anal. Chem. 91, 797–802.
Lin, H., Jang, M., Suslick, K.S., 2011. J. Am. Chem. Soc. 133, 16786–16789.
Liu, C.C., Mack, A.V., Tsao, M.-L., Mills, J.H., Lee, H.S., Choe, H., Farzan, M., Schultz, P. G., Smider, V.V., 2008. Proc. Natl. Acad. Sci. Unit. States Am. 105, 17688–17693.
Liu, B., Zhuang, J., Wei, G., 2020. Environ. Sci. Nano 7, 2195–2213.
Marvin, D.A., Welsh, L.C., Symmons, M.F., Scott, W.R.P., Straus, S.K., 2006. J. Mol. Biol. 355, 294–309.
Merzlyak, A., Indrakanti, S., Lee, S.-W., 2009. Nano Lett. 9, 846–852.
Moon, J.-S., Lee, Y., Shin, D.-M., Kim, C., Kim, W.-G., Park, M., Han, J., Song, H., Kim, K., Oh, J.-W., 2016. Chem. Asian J. 11, 3097–3101.
Murugathas, T., Zheng, H.Y., Colbert, D., Kralicek, A.V., Carraher, C., Plank, N.O.V., 2019. ACS Appl. Mater. Interfaces 11, 9530–9538.
Murugathas, T., Hamiaux, C., Colbert, D., Kralicek, A.V., Plank, N.O.V., Carraher, C., 2020. ACS Appl. Electron. Mater. 2, 3610–3617.
Oh, J.-W., Chung, W.-J., Heo, K., Jin, H.-E., Lee, B.Y., Wang, E., Zueger, C., Wong, W., Meyer, J., Kim, C., Lee, S.-Y., Kim, W.-G., Zemla, M., Auer, M., Hexemer, A., Lee, S.-W., 2014. Nat. Commun. 5, 3043.
Park, J., Lee, J.-M., Chun, H., Lee, Y., Hong, S.J., Jung, H., Kim, Y.-J., Kim, W.-G., Devaraj, V., Choi, E.J., Oh, J.-W., Han, B., 2021. Biosens. Bioelectron. 177, 112979.
Parmley, S.F., Smith, G.P., 1989. Filamentous fusion phage cloning vectors for the study of epitopes and design of vaccines. In: Atassi, M.Z. (Ed.), Immunobiology of Proteins and Peptides V. Springer US, Boston, MA, pp. 215–218.
Santos, F.J., Galceran, M.T., 2003. J. Chromatogr. A 1000, 125–151.
Scott, J., Smith, G., 1990. Science 249, 386–390.
Smith, G., 1985. Science 228, 1315–1317.
Smith, G.P., Petrenko, V.A., 1997. Chem. Rev. 97, 391–410.
Song, J., Gardner, B.D., Holland, J.F., Beaudry, R.M., 1997. J. Agric. Food Chem. 45, 1801–1807.
Suslick, B.A., Feng, L., Suslick, K.S., 2010. Anal. Chem. 82, 2067–2073.
Tian, F., Tsao, M.-L., Schultz, P.G., 2004. J. Am. Chem. Soc. 126, 15962–15963.
Yang, H., Kim, D., Kim, J., Moon, D., Song, H.S., Lee, M., Hong, S., Park, T.H., 2017. ACS Nano 11, 11847–11855.
Yoo, Y.J., Kim, W., Ko, J.H., Kim, Y.J., Lee, Y., Stanciu, S.G., Lee, J., Kim, S., Oh, J., Song, Y.M., 2020. Adv. Sci. 7, 2000978.
Yu, Q., Xu, S., Shi, W., Tian, Y., Wang, X., 2020. Anal. Methods 12, 1852–1857.

Zhang, C., Bailey, D.P., Suslick, K.S., 2006. J. Agric. Food Chem. 54, 4925–4931.
Zhang, C., Suslick, K.S., 2007. J. Agric. Food Chem. 55, 237–242.
Zhu, J., Xiao, Z., 2019. Eur. Food Res. Technol. 245, 129–141.